

Supplemental material for "Brownian Integrated Covariance Functions for Gaussian Process Modeling: Sigmoidal Versus Localized Basis Functions" by Ning Zhang and Daniel W. Apley

Additional Basis Functions and GRF Realizations

Figures S1—S4 of this supplement show additional basis functions and GRF realizations, analogous to those shown in Figures 4 and 5 of the paper. Results for the PEXP and FBF models are in Figures S1 and S2, respectively, and results for the BIPEXP model are in Figures S3 and S4. Figure S3 shows the effects of ν and ϕ for $p = 1$, and Figure S4 shows the effects of p . As in Figures 4 and 5, to provide a more common basis for comparison, the PEXP basis functions plotted in Figure S1 are also the conditional covariance function $g_i(\mathbf{x}) = \text{Cov}[Y(\mathbf{x}), Y(\mathbf{x}_i) | Y(\mathbf{0}) = 0] = R(\mathbf{x}, \mathbf{x}_i) - R(\mathbf{x}, \mathbf{0})R(\mathbf{x}_i, \mathbf{0})/R(\mathbf{0}, \mathbf{0})$, where $R(\mathbf{x}, \mathbf{x}')$ is the usual PEXP covariance function given by (1). Notice that, as the scale parameter $\phi \rightarrow \infty$, the colored GRF $C(\mathbf{z})$ in the definition of the BI covariance model (7) approaches white noise, in which case the BI covariance model approaches the FBF covariance model with the same p . We can begin to see this for the largest value of ϕ (the $\{p = 1, \nu = 1.95, \phi = 3\}$ case) in Figure S3.

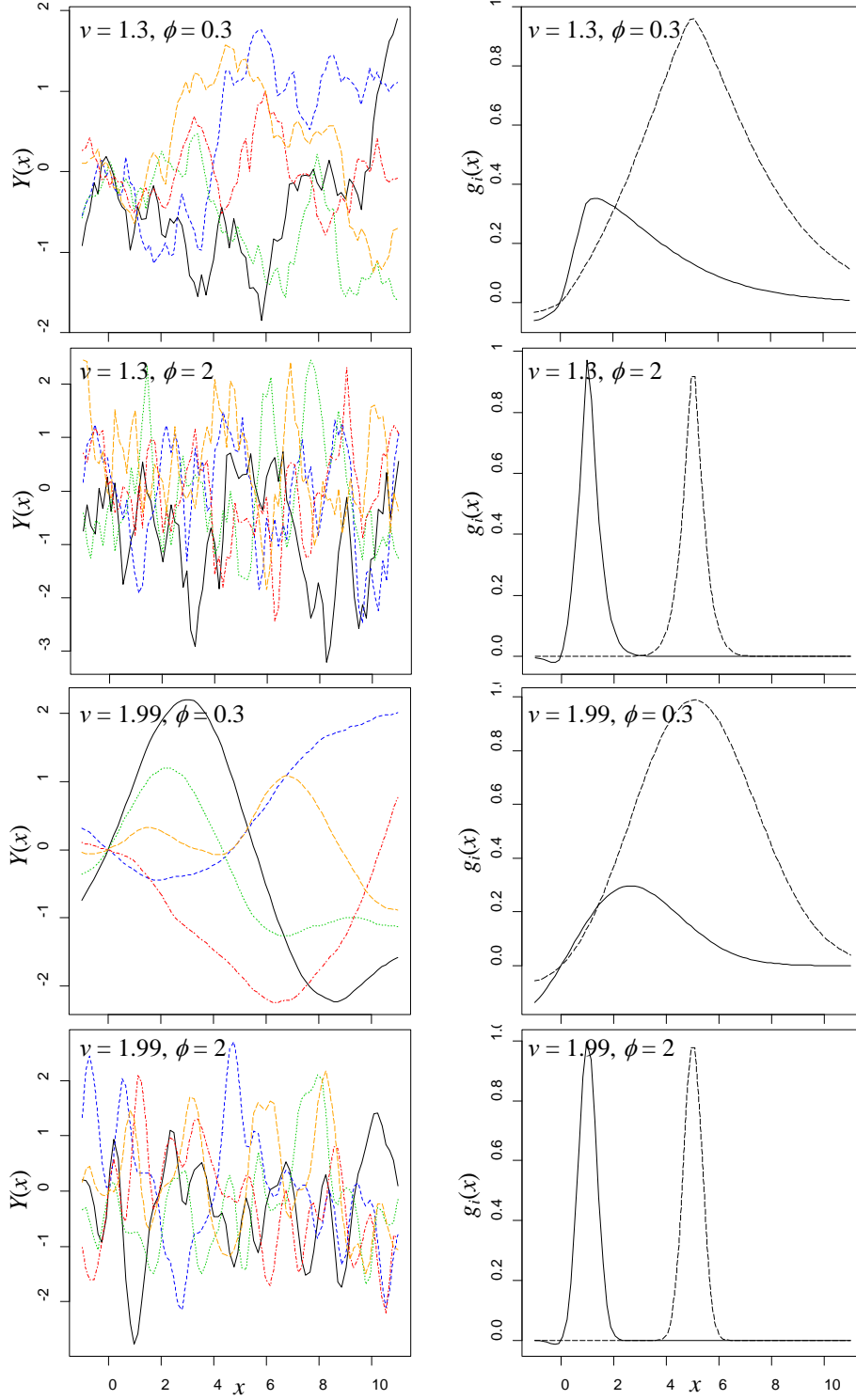


Figure S1. Examples of five random realizations of $Y(x)$ (left column) and two basis functions $g_i(x)$ (right column) for PEXP models with $d = 1$, and various $\{\nu, \phi\}$. The two basis functions are for $x_i = 1$ (solid line) and $x_i = 5$ (dashed line).

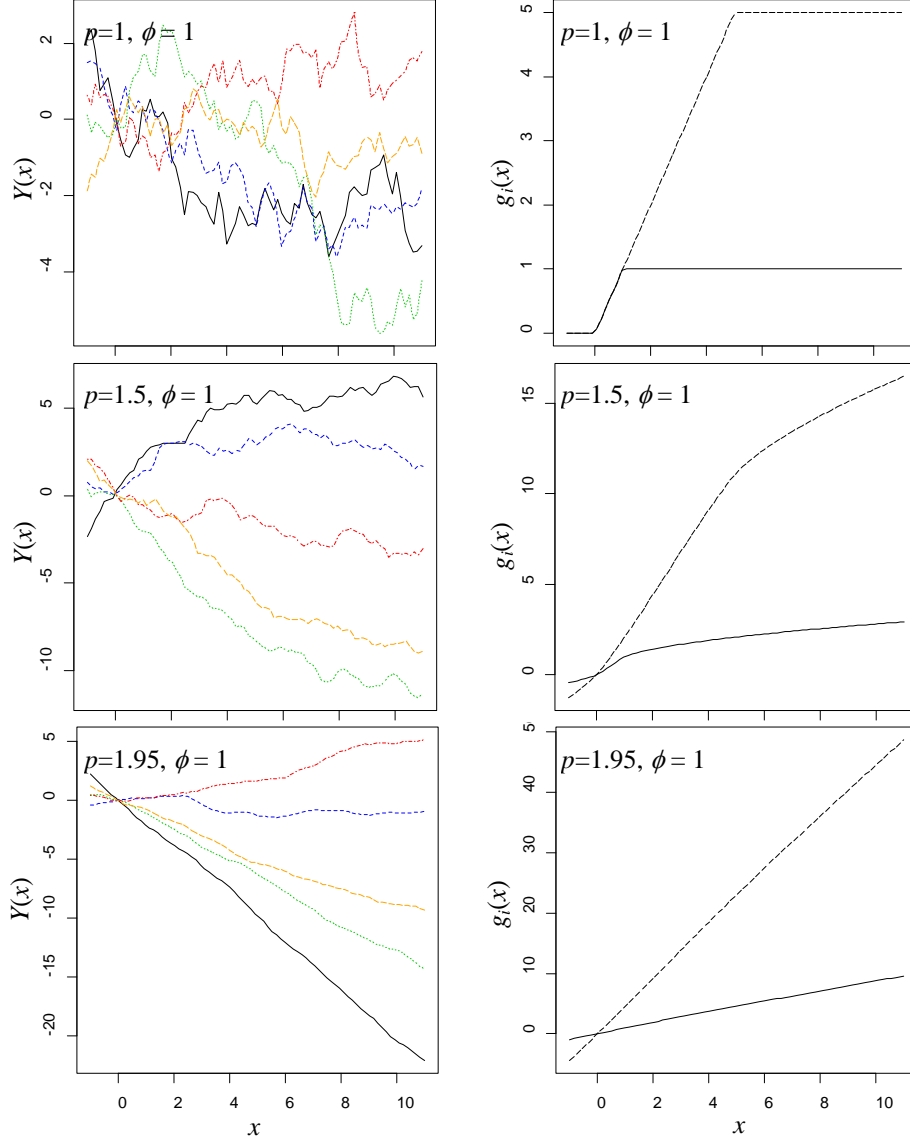


Figure S2. Examples of five random realizations of $Y(x)$ (left column) and two basis functions $g_i(x)$ (right column) for FBF models with $d = 1$, $\phi = 1$, and various p . The two basis functions are for $x_i = 1$ (solid line) and $x_i = 5$ (dashed line).

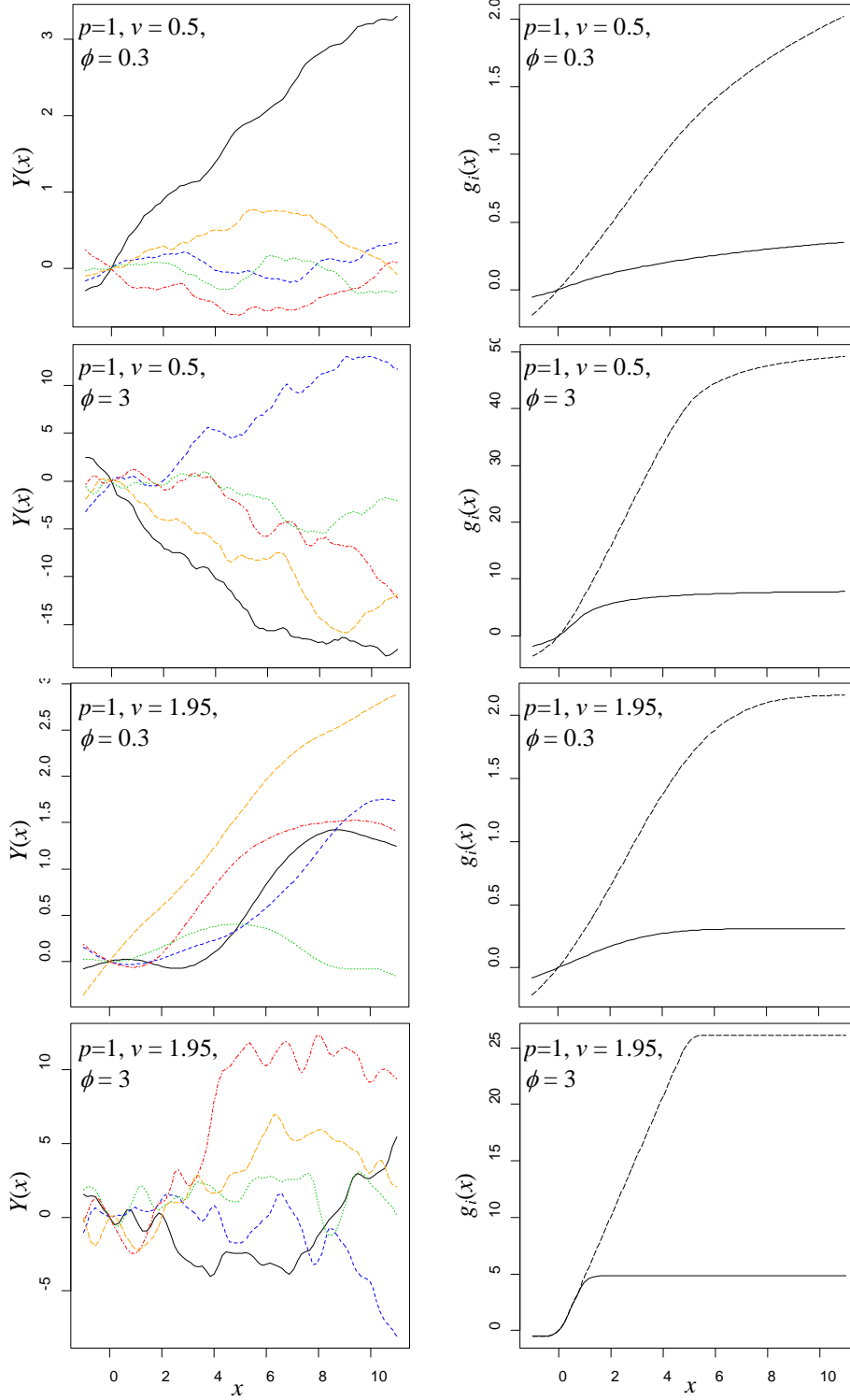


Figure S3. Examples of five random realizations of $Y(x)$ (left column) and two basis functions $g_i(x)$ (right column) for BIPEXP models with $d=1$, $p=1$, and various $\{v, \phi\}$. The two basis functions are for $x_i=1$ (solid line) and $x_i=5$ (dashed line).

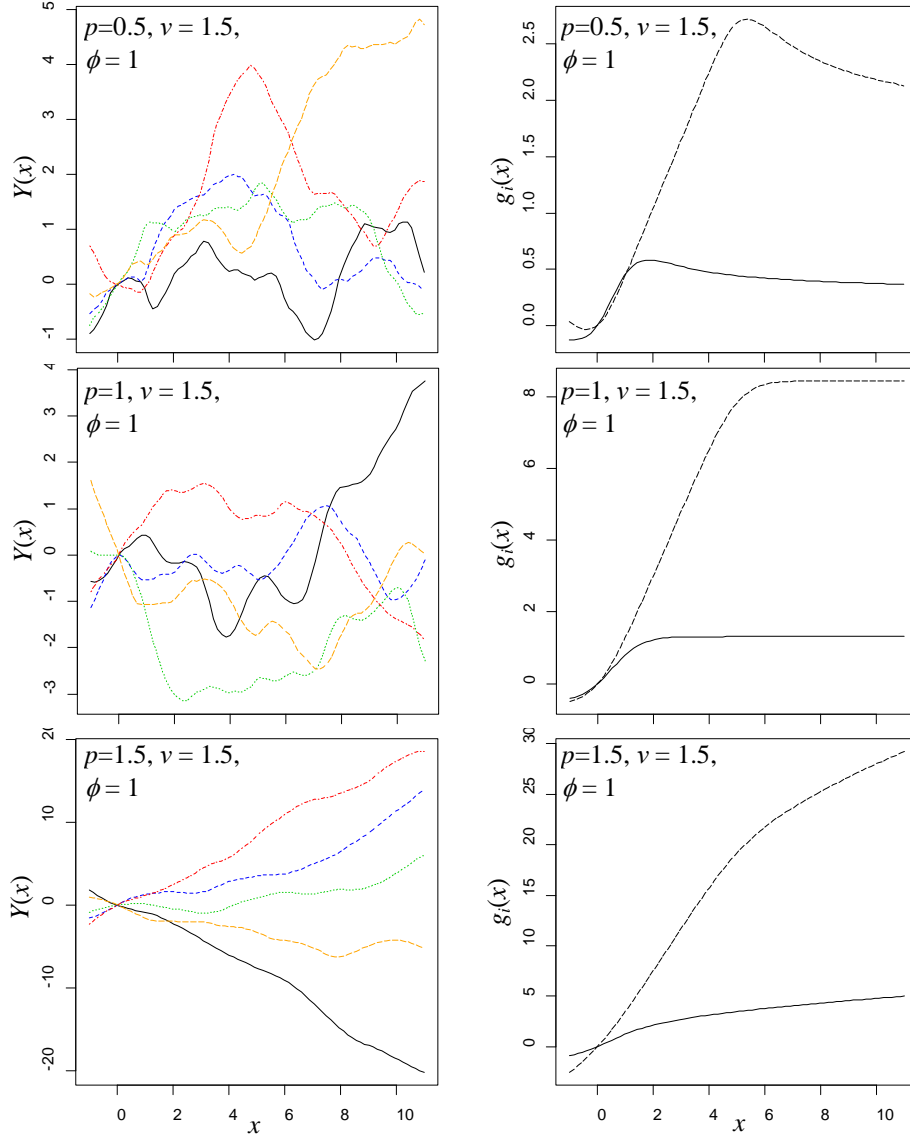


Figure S4. Examples of five random realizations of $Y(x)$ (left column) and two basis functions $g_i(x)$ (right column) for BIPEXP models with $d = 1$, $\nu = 1$, $\phi = 1$, and various p . The two basis functions are for $x_i = 1$ (solid line) and $x_i = 5$ (dashed line).

Details of the Examples in Section 4.4

This section provides details on the examples used in Section 4.4 to compare the BIPEXP and PEXP performances. Four examples use models of real physical systems, and the remaining examples use mathematical test functions. In each of the examples, the PEXP and BIPEXP models were fit to a set of data from one or more designed experiments, and the fitted models were then used to predict the response values at a separate set of test sites. The test prediction

root mean square error (RMSE) results are summarized in Table 1 for the real examples and in Table 2 for the mathematical test functions. We first describe the four real examples.

Heat Exchanger Example. Qian, Seepersad, Joseph, Allen and Wu (2006) presented an example in which the thermal conditions of a heat exchanger in an electronic cooling application are simulated. The $d = 4$ input variables are the mass flow rate of entry air (x_1), temperature of entry air (x_2), temperature of the heat source (x_3), and solid material thermal conductivity (x_4). The output of the simulation is the heat transfer rate y . Details of the simulation can be found in Qian, et al. (2006). They conducted a 64-run orthogonal array-based Latin hypercube design (LHD) to fit the kriging predictor, and they chose another 14 test runs randomly over a region slightly larger than the original design space to validate the predictor. Fitting a Gaussian covariance model (the PEXP model was virtually identical, because the MLE of the PEXP ν was 1.99) to the LHD data gives MLEs of $\hat{\phi}_1 = 0.4695$, $\hat{\phi}_2 = 2.0913$, $\hat{\phi}_3 = 0.3777$, $\hat{\phi}_4 = 2.6914$, $\hat{\mu} = 20.2426$, $\hat{\sigma}^2 = 64.2167$, and the test RMSE is 5.148, which agrees with the results stated in Qian, et al. (2006). For the BIPEXP covariance model, the MLEs were $\hat{\phi}_1 = 7.0065$, $\hat{\phi}_2 = 6.5739$, $\hat{\phi}_3 = 4.8681$, $\hat{\phi}_4 = 2.4039$, $\hat{\sigma}^2 = 0.9208$, $\hat{\nu} = 1.9999$, and $\hat{p} = 1.8559$, and the test RMSE was 2.157, which is less than half that of the PEXP model.

The sample standard deviation of the 14 test response values was $SD(y) = 9.827$, so the ratio $RMSE/SD(y)$ is 0.524 for the PEXP model, versus 0.220 for the BIPEXP model. Consequently, the test r^2 value is $r^2 = 1 - [RMSE/SD(y)]^2 = 0.726$ for the PEXP model, versus 0.952 for the BIPEXP model. Notice that $RMSE/SD(y)$ represents the ratio of the test error standard deviation (RMSE) to the standard deviation of the response observations. We prefer this ratio over r^2 as a measure of fit, because r^2 can be misleading when modeling deterministic computer experiments. For example, an r^2 of 0.99 is considered a nearly perfect fit in many regression modeling contexts, but not necessarily for modeling deterministic computer experiments. As a point of reference, r^2 is 0.9659 for the fit in Figure 1(a) and 0.9854 for the fit in Figure 3.

Borehole example. The borehole example is a higher-dimensional example ($d = 8$) that was introduced by Morris, Mitchell and Ylvisaker (1993). The flow rate (y) of water through a borehole that is drilled from the ground surface through two aquifers is modeled as

$$y = \frac{2\pi T_u(H_u - H_l)}{\ln\left(\frac{r}{r_w}\right) \left[1 + \frac{2LT_u}{\ln\left(\frac{r}{r_w}\right)r_w^2 K_w} + \frac{T_u}{T_l} \right]},$$

where the eight variables are the radius r_w (x_1) of the borehole, the radius r (x_2) of influence, the transmissivity T_u (x_3) of the upper aquifer, the potentiometric head H_u (x_4) of the upper aquifer, the transmissivity T_l (x_5) of the lower aquifer, the potentiometric head H_l (x_6) of the lower aquifer, the length L (x_7) of the borehole, and the hydraulic conductivity K_w (x_8) of the borehole. Morris, et al. (1993) give details of the model and the ranges of the input variables.

Joseph, Hung and Sudjianto (2008) used a 27-run, three-level orthogonal array design for the borehole example. The MLEs for models fit to the data for this design were $\hat{\phi}_1 = 0.144$, $\hat{\phi}_2 = 9.59 \times 10^{-12}$, $\hat{\phi}_3 = 5.44 \times 10^{-8}$, $\hat{\phi}_4 = 0.00981$, $\hat{\phi}_5 = 6.37 \times 10^{-5}$, $\hat{\phi}_6 = 0.0141$, $\hat{\phi}_7 = 0.0161$, $\hat{\phi}_8 = 1.65 \times 10^{-3}$, $\hat{\nu} = 2$, $\hat{\mu} = 138.9771$, and $\hat{\sigma}^2 = 2.4611 \times 10^4$ for the PEXP model and $\hat{\phi}_1 = 4.08$, $\hat{\phi}_2 = 0.0150$, $\hat{\phi}_3 = 0.0115$, $\hat{\phi}_4 = 1.21$, $\hat{\phi}_5 = 0.0266$, $\hat{\phi}_6 = 1.02$, $\hat{\phi}_7 = 1.54$, $\hat{\phi}_8 = 0.677$, $\hat{\nu} = 1.00$, $\hat{p} = 1.12$ and $\hat{\sigma}^2 = 0.0055$ for the BIPEXP model. Notice that the PEXP model reduced to a Gaussian covariance model ($\hat{\nu} = 2$) for this example, which is consistent with the fact that the borehole response surface is known to be quite smooth. To serve as test sites, we also used a 5,000-run LHD over the same input domain. The test RMSE for the PEXP model was 4.645 ($r^2 = 0.9894$, RMSE/SD(y) = 0.1030), versus a much lower test RMSE of 1.685 ($r^2 = 0.9986$, RMSE/SD(y) = 0.0374) for the BIPEXP model.

We also considered 27-run LHDs for the borehole example. We generated 100 different 27-run LHDs, and for each, we fit a PEXP model and a BIPEXP model. The average test RMSEs over the 100 different designs were 3.295 for the PEXP model, versus 2.507 for the BIPEXP model. Zhang and Apley (2014) found that the FBF model performed worse than the PEXP model for the borehole example with LHDs, and they concluded that this was because the FBF

model has difficulty in handling smooth response surfaces. The fact that the BIPEXP model performed even better than the PEXP model for this borehole example indicates that, unlike the FBF model, it is capable of handling smooth response surfaces.

G-protein example. The G-protein model is a biosystems model for the ligand activation of G-protein in yeast and is described in detail in Yi, et al. (2005). The model consists of a system of ordinary differential equations (ODEs)

$$\begin{aligned}\dot{\eta}_1 &= -u_1\eta_1x + u_2\eta_2 - u_3\eta_1 + u_5 \\ \dot{\eta}_2 &= u_1\eta_1x - u_2\eta_2 - u_4\eta_2 \\ \dot{\eta}_3 &= -u_6\eta_2\eta_3 + u_8(G_{\text{tot}} - \eta_3 - \eta_4)(G_{\text{tot}} - \eta_3) \\ \dot{\eta}_4 &= u_6\eta_2\eta_3 - u_7\eta_4 \\ y &= (G_{\text{tot}} - \eta_3)/G_{\text{tot}}\end{aligned}$$

where the nine input variables are the concentration x of ligand and a set $\{u_1, \dots, u_8\}$ of eight kinetic parameters, and the response is the normalized concentration y of part of the complex. The total concentration G_{tot} of G-protein complex after 30 seconds is treated as a known parameter. The concentrations $\{\eta_1, \dots, \eta_4\}$ of four chemical species are determined internally in the simulation, and $\dot{\eta}_j \equiv \partial\eta_j/\partial t$.

Loeppky, Sacks and Welch (2009) developed computer code to solve the system of ODEs, and Jerome Sacks provided to us a set of data that were generated from the code as follows. Five of the nine input variables were held fixed, and the other four $\{x, u_1, u_6, u_7\}$ were treated as the experimental inputs ($d = 4$), after transforming to log-scale and then normalizing to the interval $[0, 1]$. A 41-run maximin LHD served as the design data, and a separate 1000-run maximin LHD served as the test data. The ODE solver calculated the response values at each of the training and test sites. To the 41-run LHD we fit a PEXP model, for which the MLEs were $\hat{v} = 1.9998$, $\hat{\phi}_1 = 0.3632$, $\hat{\phi}_2 = 0.6675$, $\hat{\phi}_3 = 0.7130$, $\hat{\phi}_4 = 1.4399$, $\hat{\mu} = 0.3758$, $\hat{\sigma}^2 = 0.1291$, and the test RMSE was 0.0162 ($r^2 = 0.9940$, $\text{RMSE}/\text{SD}(y) = 0.0775$). We also fit a BIPEXP model, for which the MLEs were $\hat{v} = 2$, $\hat{p} = 1$, $\hat{\phi}_1 = 0.4672$, $\hat{\phi}_2 = 0.7784$, $\hat{\phi}_3 = 0.7882$, $\hat{\phi}_4 = 1.4135$, $\hat{\sigma}^2 = 0.0095$, and the test RMSE was 0.0145 ($r^2 = 0.9952$, $\text{RMSE}/\text{SD}(y) = 0.0693$).

Nilson-Kuusk example. This is an analytical reflectance model for a homogeneous plant canopy, which was introduced in Nilson and Kuusk (1989). We used the data from Bastos and O’Hagan (2009), which were produced via a simulation with five input variables ($d = 5$), each of which was scaled to the interval $[0, 1]$. The data are for two independent LHDs, one having 100 runs, and the other having 150 runs. We first fit a PEXP covariance model to the 100-run LHD, for which the MLEs were $\hat{\nu} = 1.8845$, $\hat{\phi}_1 = 0.2196$, $\hat{\phi}_2 = 0.1521$, $\hat{\phi}_3 = 0.0151$, $\hat{\phi}_4 = 0.7286$, $\hat{\phi}_5 = 0.5506$, $\hat{\mu} = 0.1778$, $\hat{\sigma}^2 = 0.0321$, and the RMSE over the 150-run LHD was 0.0187 ($r^2 = 0.9918$, $\text{RMSE}/\text{SD}(y) = 0.0903$). A Gaussian covariance model performed worse, resulting in a test RMSE of 0.0251 ($r^2 = 0.9853$, $\text{RMSE}/\text{SD}(y) = 0.1212$). We also fit a BIPEXP model, for which the MLEs were $\hat{\nu} = 1$, $\hat{p} = 1.0855$, $\hat{\phi}_1 = 6.2696$, $\hat{\phi}_2 = 2.8906$, $\hat{\phi}_3 = 0.6210$, $\hat{\phi}_4 = 0.3922$, $\hat{\phi}_5 = 16.5217$, $\hat{\sigma}^2 = 8.3752 \times 10^{-6}$, and the test RMSE was 0.0183 ($r^2 = 0.9922$, $\text{RMSE}/\text{SD}(y) = 0.0883$).

We then repeated the analysis but with the training and test data reversed. For the PEXP model fit to the 150-run LHD, the MLEs were $\hat{\nu} = 1.8443$, $\hat{\phi}_1 = 0.2118$, $\hat{\phi}_2 = 0.1582$, $\hat{\phi}_3 = 0.0268$, $\hat{\phi}_4 = 0.0162$, $\hat{\phi}_5 = 0.6569$, $\hat{\mu} = 0.1851$, $\hat{\sigma}^2 = 0.0285$, and the test RMSE over the 100-run LHD was 0.0169 ($r^2 = 0.9929$, $\text{RMSE}/\text{SD}(y) = 0.0843$). The results of using a Gaussian covariance model were again worse, with a test RMSE of 0.0192 ($r^2 = 0.9908$, $\text{RMSE}/\text{SD}(y) = 0.0959$). For the BIPEXP model, the MLEs were $\hat{\nu} = 1.2252$, $\hat{p} = 1.4169$, $\hat{\phi}_1 = 4.5639$, $\hat{\phi}_2 = 3.4626$, $\hat{\phi}_3 = 0.5428$, $\hat{\phi}_4 = 0.4914$, $\hat{\phi}_5 = 16.8493$, $\hat{\sigma}^2 = 1.7703 \times 10^{-5}$, and the test RMSE was 0.0168 ($r^2 = 0.9931$, $\text{RMSE}/\text{SD}(y) = 0.0831$).

The results for all of the preceding examples are summarized in Table 1 of the paper, which shows the test RMSEs, the ratio of test RMSE to $\text{SD}(y)$, and the percent improvement in test RMSE for the BIPEXP model. The latter is defined as $(\text{RMSE}_{\text{PEXP}} - \text{RMSE}_{\text{BIPEXP}})/\text{RMSE}_{\text{PEXP}} \times 100$. Across these real examples, the BIPEXP had test RMSE that was between 0.6% and 63.7% better than the PEXP test RMSE.

In addition to the real examples in Table 1, we also compared the BIPEXP and PEXP performances for a number of mathematical test functions that have been considered in the prior

literature. Table S1 lists the test functions, prior work that has considered the function (and from which further details can be found), and the input domain (a rectangular region in each case) for the experiment. For each function, we averaged the test RMSE across 100 replicates. On each replicate we generated a different LHD design, fit PEXP and BIPEXP models to the data for the design, and then calculated the test RMSE for 1,600 test sites that were evenly spaced over the input domain. For Function 3, 48-run LHDs were used. For all other functions, 24-run LHDs were used. More runs were used for Function 3, because it was more difficult to model. Table 2 of the paper summarizes the results for the mathematical test functions in Table S1, including the Xiong et al. (2007) example from Figures 1 and 3.

Function # (reference)	Function, $y(\mathbf{x}) =$	input domain
Function 1 (Currin et al., 1999)	$\left[1 - \exp\left(-\frac{1}{2x_2}\right)\right] \cdot \frac{2300x_1^3 + 1900x_1^2 + 2092x_1 + 60}{100x_1^3 + 500x_1^2 + 4x_1 + 20}$	$x_1, x_2 \in [0,1]$
Function 2 (Sasena et al., 2002)	$2 + 0.01(x_2 - x_1^2)^2 + (1 - x_1)^2 + 2(2 - x_2)^2 + 7 \sin(0.5x_1) \sin(0.7x_1x_2)$	$x_1, x_2 \in [0,5]$
Function 3 (Paciorek, 2003)	$1.9 \cdot \{1.35 + \exp(x_1) \cdot \sin[13(x_1 - 0.6)^2] \cdot \exp(-x_2) \cdot \sin(7x_2)\}$	$x_1, x_2 \in [0,1]$
Function 4 (Xiong et al., 2007)	$x_1 \cdot \exp(-x_1^2 - x_2^2)$	$x_1, x_2 \in [-2.5, 2.5]$
Function 5 (Paciorek, 2003)	$\sin\left(\frac{1}{x_1x_2}\right)$	$x_1, x_2 \in [0.3, 1]$
Function 6 (Osio et al., 1996)	$\cos[6(x_1 - 0.5)] + 3.1 x_1 - 0.7 + 2(x_1 - 0.5) + \sin\left[\frac{1}{ x_1 - 0.5 + 0.31}\right] + 0.5x_2$	$x_1, x_2 \in [0,1]$
Function 7 (Jin et al., 1996)	$\left(x_2 - \frac{5.1}{4\pi^2}x_1^2 + \frac{5}{\pi}x_1 - 6\right)^2 + 10\left(1 - \frac{1}{8\pi}\right)\cos x_1 + 10$	$x_1 \in [-5, 10]$ $x_2 \in [0, 15]$
Function 8 (Hardy, 1975)	$\left(4 - 2.1x_1^2 + \frac{x_2^3}{3}\right)x_1^2 + x_1x_2 + (-4 + 4x_2^2)x_2^2$	$x_1, x_2 \in [-10, 10]$
Function 9 (Jin et al., 1996)	$[1 + (x_1 + x_2 + 1)^2(19 - 14x_1 + 3x_1^2 - 14x_2 + 6x_1x_2 + 3x_2^2)] \cdot [30 + (2x_1 - 3x_2)^2(18 - 32x_1 + 12x_1^2 + 48x_2 - 36x_1x_2 + 27x_2^2)]$	$x_1, x_2 \in [-2, 2]$

Table S1. Mathematical test functions and experimental designs used to compare the PEXP and BIPEXP models.

Relationship between the PEXP and BIPEXP Models

When comparing the performance of the PEXP and the BIPEXP models, one situation that favors the PEXP model is when the true response surface is a realization of a GRF whose

covariance function is truly PEXP. In this section we show that the BIPEXP model with p restricted to $[1, 2)$ does almost as well as the PEXP in this situation, and we draw a loose connection between the PEXP model and the BIPEXP model when p is close to zero.

Consider the $d = 1$ case and an input domain of $[0, 1]$. We conducted a Monte Carlo simulation in which, on each replicate, a different true response surface was generated, the PEXP and BIPEXP models were fit to a set of training points on the surface, and then the two models were used to predict a set of test points on the same surface. For each replicate, the training and test data on the response surface were generated from a PEXP covariance model with $\mu = 0$ and the parameters ν and θ randomly generated (as different values on each replicate) from a uniform distribution over the intervals $[1, 2]$ and $[1, 6]$, respectively. The training data were the response observations at n evenly spaced input sites over the interval $[0, 1]$, and the test data were the response observations at 100 evenly spaced input locations over the interval $[0, 1]$. For each replicate, the parameters of both models were fitted using MLE, and the RMSEs for predicting the 100 test sites for both models were calculated. The average RMSE values, and their standard errors, over the 100 Monte Carlo replicates are shown in Table 4 for six different values of n (5, 10, 15, 20, 25, and 30). For larger values of n , both methods experienced numerical difficulties when inverting \mathbf{R} . The "Difference" column in Table S2 is the average RMSE for the PEXP model minus the average RMSE for the BIPEXP model. Because the two models were fit to the same randomly generated surface on each replicate, there is an inherent pairing that results in the standard error of the average difference being substantially less than the standard errors of the average RMSEs for the two models.

Overall, Table S2 indicates that the two models perform quite similarly when the true response surface is generated as a PEXP random field. For larger n (e.g., above 25), the PEXP model performs slightly better than the BIPEXP model, as one would expect. Somewhat surprisingly, the BIPEXP model actually performs better than the PEXP model for $n < 20$. This is most likely because the covariance parameters were estimated. If the true covariance parameters (i.e., the same ones that were used to generate the response surface) were treated as

known and used in the PEXP model when predicting the test points, then the PEXP model would obviously have outperformed any other model, because the kriging predictor is defined as the best linear unbiased predictor. That the BIEXP model performed better when the parameters were estimated is some indication that it is more robust to parameter estimation errors.

n	PEXP Model		BIEXP Model		Difference
	RMSE	RMSE/SD(Y)	RMSE	RMSE/SD(Y)	RMSE
5	0.4119 (0.0232)	69.32%	0.3315 (0.0161)	56.12%	0.0805 (0.0135)
10	0.1878 (0.0137)	31.31%	0.1743 (0.0114)	28.47%	0.0135 (0.0047)
15	0.1384 (0.0090)	23.88%	0.1362 (0.0085)	23.25%	0.0022 (0.0018)
20	0.1104 (0.0073)	17.36%	0.1102 (0.0072)	17.30%	0.0002 (0.0003)
25	0.0995 (0.0071)	15.22%	0.0999 (0.0071)	15.29%	-0.0005 (0.0002)
30	0.0862 (0.0067)	13.53%	0.0926 (0.0078)	14.51%	-0.0065 (0.0020)

Table S2. Comparison of test RMSE values (standard errors are in parentheses) for the PEXP and BIEXP models when the true surface is generated as a random field with PEXP covariance.

When we repeated the preceding Monte Carlo simulation using a lower bound of zero for p (in the preceding, the lower bound for p was 1.0), we obtained slightly better average RMSE results for the BIEXP model. The average value of \hat{p} for the BIEXP model was quite small (0.1554), and \hat{p} was less than 0.2 on 80% of the replicates. Consequently, the behavior of a BI GRF when p is close to zero may be of some interest. To investigate this, rewrite (7) as

$$B_p^C(\mathbf{x}) = \int_{\mathbb{R}^d} k_{p,d} f_{p,x}(\mathbf{z}) C(\mathbf{z}) d\mathbf{z}, \quad (\text{S1})$$

where we have defined the function $f_{p,x}(\mathbf{z}) = \|\mathbf{x} - \mathbf{z}\|^{(p-d)/2} - \|\mathbf{z}\|^{(p-d)/2}$. Figure 8 plots $f_{p,x}(z)$ as a function of z for various p for the case that $d = 1$ and $x = 6$. Notice that $f_{p,x}(z) = \pm\infty$ at $z = \{0, x\}$ for $d = 1$ and $p < 1$. Figure 8 indicates that for small p , $f_{p,x}(z)$ bears some resemblance to the difference between two impulse functions, one at $z = x$ and the other at $z = 0$. If we approximate $f_{p,x}(z)$ by these two impulse functions, then the integral in (S1) can be approximated as $B_p^C(x) \approx C(x) - C(0)$ (aside from a constant multiplicative factor), which is the same as the underlying stationary random field $C(\mathbf{x})$, except that the value of $C(\bullet)$ at the origin is subtracted to preserve the condition that $B_p^C(\mathbf{0}) = 0$. This may partly explain why the

BIPEXP basis functions for $p = 0.5$ in Figure 7 are more peaked than for larger p and, in this regard, are more similar to the PEXP basis functions.

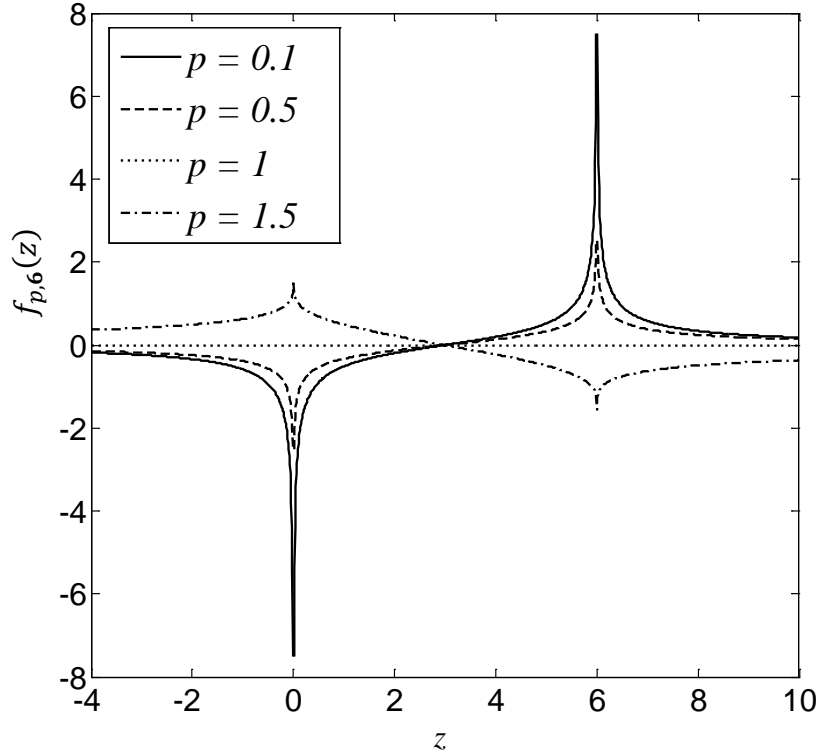


Figure 8. Plot of $f_{p,x}(z)$ versus z for $d = 1$, $x = 6$ and various p .

Although the BIPEXP model had slightly better test RMSE in the preceding example when the lower bound on p was reduced below 1, we still recommend restricting p to the interval $[1, 2)$. When p is close to zero, the numerical integration for calculating $R_B(\mathbf{x}, \mathbf{x}')$ can become poorly conditioned. The primary advantage of allowing a smaller p may be that the BIPEXP model can better mimic the behavior of the PEXP model, which may be beneficial in the event that the response surface is well modeled as PEXP. However, a more reasonable approach may be to fit both a PEXP model and a BIPEXP model, with p for the latter restricted to the interval $[1, 2)$, and then to choose the better of the two models.

Computation of the Hypergeometric Function Used in (14)

To simplify the notation, consider a fixed p , H and r , and define

$$f(d) = F\left(\frac{d-1}{2}, -\frac{p}{2}; d-1; \frac{4Hr}{(H+r)^2}\right).$$

The hypergeometric function needed in (14) is $f(d)$, and this is only needed for odd $d \geq 3$. For $d = 3$ and 5,

$$f(3) = \frac{(H+r)^{2+p} - |H-r|^{2+p}}{2Hr(2+p)(H+r)^p}, \text{ and}$$

$$f(5) = \frac{3\{(H+r)^2(H-r)^2[|H-r|^{2+p} - (H+r)^{2+p}] + Hr(2+p)[|H-r|^{4+p} + (H+r)^{4+p}]\}}{2H^3r^3(2+p)(4+p)(6+p)(H+r)^p}.$$

For any other odd $d \geq 5$, $f(d+2)$ can be calculated recursively via

$$f(d+2) = \frac{d(d-2)}{(2d-2+p)(2d+p)H^2r^2} \times \left\{ \left[-H^4 + \frac{2(3d+2p-4)}{(d-2)}H^2r^2 - r^4 \right] f(d) + [H^4 - 2H^2r^2 + r^4] f(d-2) \right\}.$$

Matlab Code for Implementing the BIPEXP model

See the Matlab files *SFBFmain9dPmse.m* (main file) and *SFBFcov9dP.m* (routine called by main file).